Int J Thermophys (2007) 28:1304–1321
DOI 10.1007/s10765-007-0257-0

Density, Surface Tension, and Viscosity of CMSX-4® Superalloy

E. Ricci · D. Giuranno · R. Novakovic ·
T. Matsushita · S. Seetharaman · R. Brooks ·
L. A. Chapman · P. N. Quested

Received: 30 November 2006 / Accepted: 15 August 2007 / Published online: 12 September 2007

Abstract The surface tension, density, and viscosity of the Ni-based superalloy CMSX-4® have been determined in the temperature ranges of 1,650–1,850 K, 1,650–1,950 K, and 1,623–1,800 K, respectively. Each property has been measured in parallel by different techniques at different participating laboratories, and the results are compared with the aim to improve the reliability of data and to identify recommended values. The following relationships have been proposed: density-ρ (T) $[\mathrm{kg \cdot m^{-3}}] = 7{,}876 - 1.23(T - 1{,}654\,\mathrm{K})$; surface tension-$\gamma(T)[\mathrm{mN \cdot m^{-1}}] = 1{,}773 - 0.56(T - 1{,}654\,\mathrm{K})$; viscosity-$\eta$ (T) $[\mathrm{mPa \cdot s}] = 8.36 - 1.82 \times 10^{-2}(T - 1{,}654\,\mathrm{K})$. For a comparison, surface-tension measurements on the Al-88.6 at% Ni liquid alloy with the same Al-content as the CMSX-4® alloy were also performed. In addition, the surface tension and density have been theoretically evaluated by different models, and subsequently compared with new experimental data as well as with those reported in the literature. The surface-tension experimental data for the liquid CMSX-4® alloy were found to be close to that of the Al-88.6 at% Ni alloy which is consistent with results from the compound formation model (CFM).

Keywords CMSX-4 superalloy · Density · Ni–Al system · Surface tension · Thermophysical properties · Viscosity

---

E. Ricci (✉) · D. Giuranno · R. Novakovic
Institute for the Energetics and Interphases, CNR, Via De Marini, 6, 16149 Genoa, Italy
e-mail: e.ricci@ge.ieni.cnr.it

T. Matsushita · S. Seetharaman
Department of Materials Science and Engineering, KTH, Stockholm, Sweden

R. Brooks · L. A. Chapman · P. N. Quested
Material Centre, NPL, Teddington, UK

1 Introduction

Reliable data on the thermophysical properties of industrial alloys in the liquid phase are of increasing importance in the modeling of industrial casting and solidification processes, welding, and surface treatments. The surface tension, density, and viscosity are important parameters in the modeling of the above processes for the prediction of defects. With the improvement of algorithms, the quality of a simulation is limited primarily by the accuracy of the input parameters characterizing the material under study. Unfortunately, the high chemical reactivity of many liquid alloys make accurate measurements of these properties impossible. It is well known that gas impurities, such as sulphur and oxygen, can dramatically influence the determination of the thermophysical properties of liquid metals and alloys [1]. The large scatter which is often found in the experimental data could, to some extent, be attributed to the presence of these impurities, mainly oxygen, in the atmosphere around the metal sample. In particular, oxygen can strongly affect the surface-tension value and its temperature coefficient even if it is present in really small quantities. This fact was experimentally confirmed on pure metals [2,3] and their alloys [4] by using different measurement techniques.

This pertains, in particular, to high-temperature melts, such as the Ni-alloys and Ti-alloys which are of considerable technological interest. Among the thermophysical properties, the surface tension, density, and viscosity of a Ni-based superalloy, referred to as CMSX-4, were measured and presented here.

Measurements have been performed in parallel at different participating laboratories in order to discern potential sources of systematic measurement errors associated with different equipment and/or methods. This approach has proved to be very useful in obtaining reliable thermophysical property data. In addition, theoretical modeling of thermophysical properties was applied, in particular, to the surface tension. An understanding of the factors influencing the compositional dependence of the surface tension, as for any other thermophysical property, is important in order to provide reasonable extrapolations of measured values to a whole range of related alloy compositions. For a proper interpretation of experimental results, the effects of compound formation were analyzed.

In this study, the surface tension of nickel-based superalloy CMSX-4® was measured by means of sessile-drop techniques at temperatures just above the liquidus and higher. The measurement of the density was performed by a levitation diffusivity technique, while that of the viscosity with an oscillating cup viscosimeter. The present study was carried out based on the technique and knowledge acquired from the previous experiments [5–7]. CMSX-4® is a nickel-based superalloy widely used in the aerospace industry for turbine blades. Despite its technological relevance, only few data on its surface tension and density are available in the literature [8–10], while for viscosity a complete lack of data was found. The experimental investigations of the surface tension of industrial alloys have been augmented by thermodynamic modeling. The effects of compound formation on the surface tension have been investigated, taking the Al–Ni binary system as a model system for this class of industrial alloys.

Table 1 Composition of the CMSX-4® alloy as received

Composition at%	Al	Ti	Cr	Co	Ni	Ta	W	Re	Mo	Oth.
Nominal	12.58	1.29	7.45	9.86	62.17	2.17	2.11	0.94	0.38	1.05
By EDS	12.00	1.35	7.57	9.94	63.32	2.14	2.26	1.08	0.34	N.D.

2 Surface Tension

The CMSX-4® alloy was supplied by courtesy of Doncaster (Germany). Energy dispersive spectroscopy (EDS) analysis performed on the alloy as received showed substantial agreement with the nominal composition (Table 1). Samples of the same batch were used by different laboratories.

The surface tension of the alloy was measured in a flow of purified inert gas by the sessile-drop method. Two different techniques were applied: the X-ray sessile-drop [5] and the large-pinned drop [7]. The experiments were performed from the liquidus temperature and above: the CMSX-4® liquidus temperature is $T_l = 1654.5 \pm 4\,\mathrm{K}$ [11].

2.1 Surface-tension Measurements by X-ray Sessile-drop Technique

The apparatus used for the X-ray sessile-drop technique consists of an X-ray image analyzer and a graphite resistance furnace [9]. A schematic diagram of the apparatus is shown in Fig. 1. The X-ray unit is a Philips BV-26 imaging system with an X-ray source of 40–105 kV. The X-ray tube has a focal spot size that could be varied between 0.6 mm and 1.5 mm. The imaging system consists of a CCD camera with digital noise reduction. An IBM pc equipped with an image acquisition card enabled recording of the X-ray images. The furnace used in the equipment was acquired from Thermal Technology Inc. (Model 1000-3500-FP20). The graphite heating elements in the furnace, rated at 20 kV A, were capable of heating the furnace to 2,573 K. The furnace was controlled by a Eurotherm temperature regulator within ±2 K using a Type B thermocouple. Quartz windows of 40 mm in diameter were provided on both sides of the furnace for the X-ray source and detector. The reaction tube inside the furnace, with an inner diameter of 70 mm, is made of recrystallized Al_2O_3. Appropriate radiation shields are provided to ensure a good even-temperature zone, the length of which was measured to be about 70 mm.

The entire system was capable of operating under vacuum, inert gas, or gas mixtures. Appropriate gas-cleaning trains have been assembled to ensure that the impurity level in argon gas is very small. The argon gas supplied by AGA Gas AB, Stockholm (99.9997 at% with < 5 ppm O_2 and < 5 ppm CO_2) was passed through silica gel and ascarite in order to remove traces of moisture and CO_2 present in the gas, respectively. Final traces of moisture in the gas were removed by passing through a column of $Mg(ClO_4)_2$. The oxygen impurity in the gas was removed by passing the gas through copper turnings at 823 K and through magnesium chips at 773 K. Earlier experiments in the Department of Materials Science and Engineering, Royal Institute of

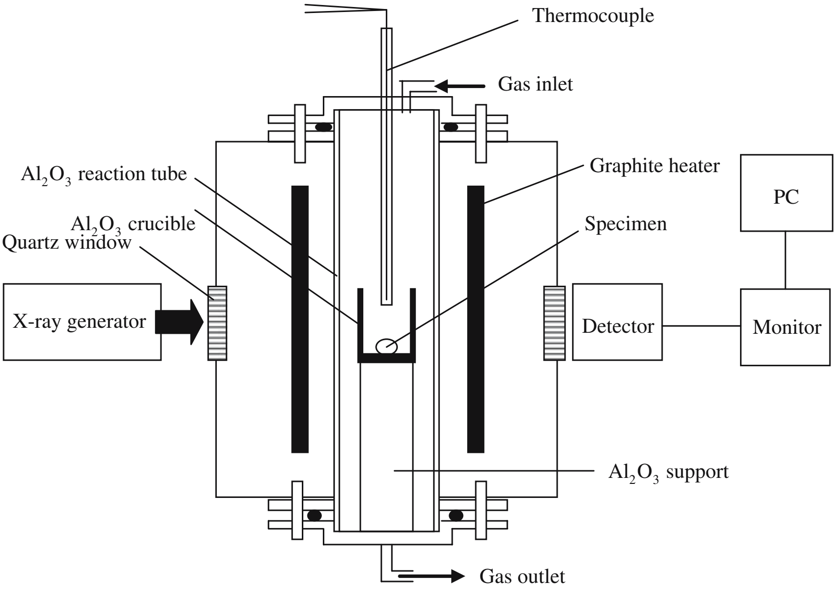

Fig. 1 Schematic diagram of the X-ray sessile-drop unit (KTH)

Technology, Stockholm have shown that these purification steps enabled the lowering of the partial pressure of oxygen in the argon gas to levels below 10^{-15} Pa. The alumina crucible with the sample was positioned on an exactly horizontal pedestal in the even-temperature zone of the furnace, in the vision field of the X-rays. The system was then evacuated and filled with purified argon gas repeatedly. The furnace was started when the oxygen partial pressure of the outgoing argon gas measured by a Ca-stabilized ZrO_2 oxygen sensor attained a value of less than 10^{-14} Pa. When the required temperature was reached, the system was allowed to equilibrate for at least 1 h before the measurements were carried out. The temperature of the samples was measured by a Pt-30%Rh/Pt-6%Rh thermocouple, which was previously calibrated. The temperature of the sample was found to be stable within ±1 K during the experiments. All the measurements were conducted by heating the samples to the maximum temperature and then performing measurements during the cooling cycles. The results were analyzed using software developed by the Department of Materials Science and Engineering, Carnegie-Mellon University, Pittsburgh, PA. The graphic part of the image analysis program, used together with this software, was developed at the Department of Materials Science and Engineering, Royal Institute of Technology, Stockholm.

2.2 Surface-tension Measurements by the Pinned-drop Method

A variant of the large-drop method [1] called the pinned-drop method [7] has been applied. In this case, the solid support is a special circular crucible with sharp edges. The design of the edges of the crucible blocks the triple line at an “apparent” contact angle that is much higher than the real one, and the axisymmetry of the drop can be imposed. A further advantage of the pinned-drop method is the high accuracy due to the large drop used; in fact, the size of the drop was chosen so that the error in surface tension did not exceed 1%.

The main experimental apparatus used consists of a tubular furnace, made up of two concentric, horizontal, alumina tubes, connected to a high vacuum line. The furnace is mounted on anti-vibration supports, and it can reach temperatures up to 1,773 K. The system can be used to work under a high vacuum (total pressure of $10^{-4}/10^{-5}$ Pa) or under controlled atmospheres such as high purity Ar (Air-Liquide Ar-N60 type, 99.9999 at% with < 0.1 ppm O_2 and < 0.1 ppm CO_2) or oxidizing atmospheres, such as He–0.2 at% O_2 mixture, as well as under reducing atmospheres as in the case of Ar-5 at% H_2 mixture. The necessary cleanliness of the environment is assured by the high quality of the materials used and a systematic procedure of backing before each experiment. A feed gas plant is also present to avoid any contamination. A high-precision flowmeter (Brooks®) and micro-leak valve (Nupro®) allow a precise and controlled amount of the gas flux inside the chamber (mean flow rate = 50 $\text{cm}^3 \cdot \text{min}^{-1}$). The operative conditions are continuously monitored. The temperature of the samples was measured by a Pt/Pt-10%Rh thermocouple, which was previously calibrated. During the measurements, the temperature of the sample was found to be stable within ±2 K. The oxygen partial pressure was monitored by using two ZrO_2 oxygen sensors (μ-gauges POAS/SETNAG®) with the Pd/PdO internal reference. The sensors measure the oxygen content in the feed and in the exhaust gas.

Samples of the CMSX-4® alloy with a mean mass of 2.5 g were mechanically abraded and chemically cleaned with an organic solvent in an ultrasonic bath. The sample was placed in a non-oriented monocrystalline alumina (sapphire) crucible ($r = 5.5$ mm). The crucible with the sample was laid on an alumina holder sliding in the experimental apparatus. When the apparatus conditioning (temperature, oxygen partial pressure) was reached, the sample was introduced into the center of the furnace by a pushrod magnetic manipulator. In this position the specimen, back-lit by a stabilized lamp, was monitored by a CCD camera (Cohu 4710). An optical bench allowed perfect alignment and uniformity of the light with the sample. In order to obtain a monochromatic light and to cut infrared emissions, optical filters were interposed between the view ports of the test chamber and the CCD camera. In addition, the chamber position can be set to insure that the crucible and the sample are horizontal. The CCD camera is equipped with standard high quality photographic lenses.

To allow measurement repeatability, the focusing, focal length, and diaphragm of the optical system were kept fixed. The acquisition frequency can be up to 10 points per second with an uncertainty up to 0.1%. For the acquisition and processing of the drop image, the IMAGING (National Instruments) system is used. The surface tension is estimated, basically, by using the nonlinear regression method proposed by Maze and Burnet [12]. The profile of the liquid drop obtained was acquired by dedicated software under the Labview® system, which can be used to obtain the surface-tension value in real time (A.S.T.R.A. view) [13]. The magnification factor was evaluated for each image used for the surface-tension measurements. Other output of particular parameters and quantities (drop volume, density, drop weight, shape factor, contact angle, etc.) can also be obtained.

At each temperature, the drop was allowed to equilibrate for a time ranging from 10 to 20 min. Measurements were done only during the stepwise cooling in order to improve reproducibility. The temperature was decreased step by step from 1,773 to 1,654 K. Sapphire crucibles were used to perform measurements both under a pure Ar-atmosphere or an Ar-5%at H_2 mixture fluxing (flow rate $3\text{L}\cdot\text{h}^{-1}$); a Ta-getter placed close to the sample was also used.

In order to compare the results obtained for the CMSX-4® commercial alloy as well as to complete the scarce experimental data on the Al–Ni alloys reported in the literature [14–16], surface-tension measurements of the Al-88.6 at% Ni liquid alloy were also performed following the same procedures adopted for the CMSX-4® commercial alloy. Both alloys have the same Al-content and thus, the Al-88.6 at% Ni alloy is relevant for a comparison with the CMSX-4® alloy.

The Al-88.6 at% Ni alloy samples were prepared by arc melting by mixing high purity nickel and aluminum (99.9999% Marz-grade). EDS analysis was performed on the alloy to check the actual composition. The pinned-drop experiments were performed following the same procedure used for the CMSX-4® alloy. Samples with a mean mass of 2 g were mechanically and chemically cleaned and then placed in a specially designed ZrO_2 crucible [7], previously treated at $T = 1{,}773$ K under high vacuum for 30 min in order to reach the stable stoichiometry of an oxygen-deficit zirconia (i.e., ZrO_{2-x}) [17]. Measurements were carried out during the stepwise cooling in the temperature range from 1,773 to 1,730 K under vacuum.

The uncertainty in the surface-tension value stems from both equipment and analysis, which is estimated to be ±2%. Density values used as input data were taken from Ref. 18.

2.3 Surface-tension Measurement Results

In the study by the X-ray sessile-drop method, two runs were conducted to confirm the reproducibility. The measurements where performed under purified argon gas. At each temperature, five to 10 X-ray pictures were taken by changing the power of the X-ray. At least two pictures showing the image most sharply were used for the analysis of the surface tension for the first and second runs. After the experiments, microscopic examination of the samples did not reveal any sign of surface oxidation.

The measurements of the surface tension of the CMSX-4® alloy by the pinned-drop method were performed under both an inert Ar-atmosphere and a reducing Ar-5%H_2 atmosphere, in the temperature range of 1,650–1,780 K. Each surface-tension value reported represents the mean value of five runs performed at each temperature. Under pure Ar, the surface-tension temperature coefficient was $\text{d}\gamma/\text{d}T = -0.25$ $\text{mN}\cdot\text{m}^{-1}\cdot\text{K}^{-1}$ and the mean value at the reference temperature was $\gamma(1,654\,\text{K}) = 1,844\,\text{mN}\cdot\text{m}^{-1}$; at temperatures higher than $T = 1,673$ K, a rapid decrease in the surface tension was observed with surface-tension values of $\gamma(1,725\,\text{K}) = 1,607\,\text{mN}\cdot\text{m}^{-1}$ and $\gamma(1,763\,\text{K}) = 1,447\,\text{mN}\cdot\text{m}^{-1}$. As a general rule, similar behavior has been observed where the sample has become contaminated with oxygen [19]. In fact, the EDS analysis performed on the surface of the CMSX-4® drop after the experiment under an Ar-atmosphere (Fig. 2a) confirmed the presence of a high

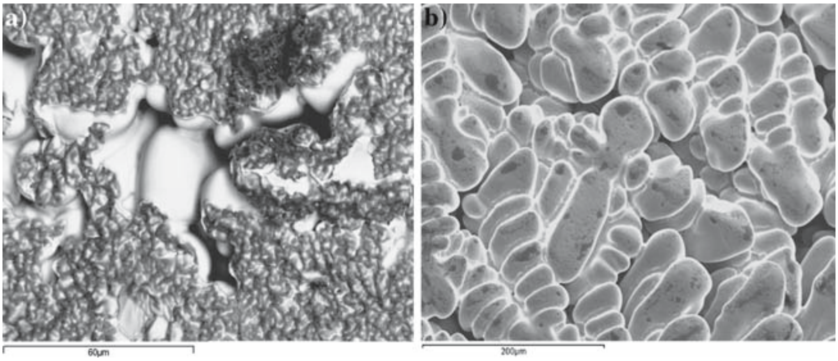

Fig. 2 SEM micrographs of the CMSX-4® drop surface after the experiments were performed (**a**) under Ar-atmosphere ($PO_2 < 10^{-3}$ Pa) and (**b**) under Ar-5%H_2-atmosphere ($PO_2 \approx 10^{-13}$ Pa)

oxygen concentration and Al-surface segregation, so that this set of data has not been considered reliable.

The experiments under an Ar-5%H_2 atmosphere were performed in the presence of a Ta-getter close to the sample. In this case, the oxygen partial pressure in the environment was $PO_2 \cong 10^{-13}$ Pa and the experimental conditions were very close to those adopted during the X-Ray sessile-drop experiments, obtained by the inert gas purification ($PO_2 \cong 10^{-15}$ Pa). After the experiment performed under such conditions, the EDS analysis of the surface of the solidified drop did not reveal the presence of oxygen or oxide film on the surface (Fig. 2b).

Experiments under a vacuum ($P_{tot} \cong 10^{-2}$ Pa), by using the same methodologies and procedures previously described, have been also carried out in both laboratories. During these experiments, a large evaporation of molten sample was observed at temperatures above 1,700 K, hampering the experiments due to the deposition of evaporated metal on the view ports. All surface-tension values obtained by the sessile-drop techniques are given in Fig. 3. It is important to mention that only the measurement at the melting point performed under vacuum has been taken into account (⋆-symbol, Fig. 3).

Figure 3 clearly shows that the surface-tension values of both laboratories obtained by the sessile-drop methods are significantly higher when compared with the values measured by the oscillating and pendant drop techniques [8], i.e., $\gamma(1{,}654\,\text{K}) = 1{,}530\,\text{mN} \cdot \text{m}^{-1}$ and $\gamma(1{,}654\,\text{K}) = 1{,}590\,\text{mN} \cdot \text{m}^{-1}$, respectively.

The presence of a reducing atmosphere and the high temperatures should allow the surface-tension measurements to be performed in oxygen-free conditions [7], due to the formation of volatile oxides leaving the liquid surface. In fact, it has been demonstrated that, from a fluid-dynamic point of view, the Knudsen regime and diffusive regime are equivalent in the definition of the oxidation/de-oxidation transition limit of a liquid metal surface [20].

An increase in the surface-tension values observed at $T < 1{,}730$ K can be attributed to the formation of stable oxide skin caused by the predominance of the segregation effect over that of evaporation at lower temperatures.

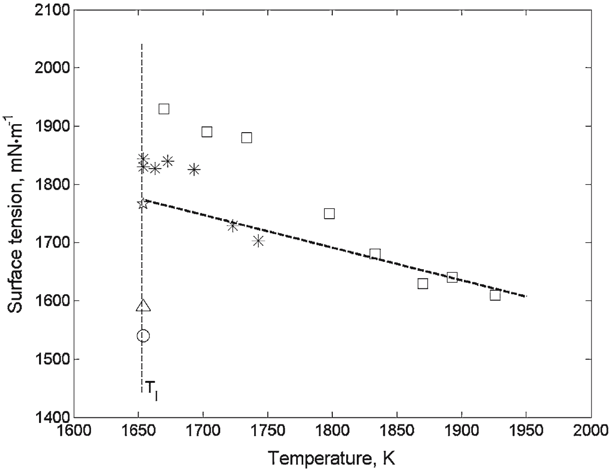

Fig. 3 Surface tension of the CMSX-4$^{®}$ alloy as a function of temperature: ($*$) pinned drop under Ar-5%H_2 atmosphere; ($\star$) pinned drop under a vacuum; (□) X-ray sessile drop; (△) oscillating drop [8]; ($\circ$) pendant drop [8]; broken line: fit of experimental data (Eq. 1 in the text). T_l is referred to as the melting temperature

Moreover, after the experiments, by visual inspection, the samples were shiny and easy detachable from the sapphire crucible demonstrating that no strong interactions occurred between the liquid metal and the crucible material. This last effect seems to contradict evidence reported in the literature [21] concerning the strong interactions occurring at the Al/Al_2O_3 interface at temperatures higher than 1,373 K.

Taking into account that no contamination came from sapphire crucibles and the effect of the oxidative-segregation occurred at lower temperatures, only the surface-tension data obtained at higher temperatures have to be considered as reliable. Thus, a more reasonable relationship of the surface tension of the CMSX-4$^{®}$ alloy as a function of temperature can be proposed (broken line in Fig. 3):

$$\gamma(T)[\mathrm{mN\cdot m^{-1}}] = 1{,}773.3 - 0.56(T - 1{,}654\,\mathrm{K}) \tag{1}$$

The temperature coefficient of Eq. 1 is close to the corresponding values for pure metals which are between -0.1 and $-0.7\,\mathrm{mN\cdot m^{-1}\cdot K^{-1}}$ [22].

The reliability of Eq. 1 can be confirmed taking into account the results obtained from the surface-tension measurements of the Al-88.6 at% Ni alloy, having the same Al-content as the commercial alloy, the object of this study. The surface tension of the Al-88.6 at% Ni alloy measured by the pinned-drop method can be described by

$$\gamma(T) = 1{,}781 - 0.40(T - 1{,}713\,\mathrm{K})[\mathrm{mN\cdot m^{-1}}] \tag{2}$$

The surface-tension value of the Al-88.6 at% Ni at $T = 1{,}913$ K, relevant for a comparison with the CMSX-4 alloy, is $\gamma(1{,}913\,\mathrm{K}) = 1{,}701\,\mathrm{mN\cdot m^{-1}}$. The value reported in the literature [15] or the alloy composition close to the previous one, Al-89.7 at% Ni, is $\gamma(1{,}913\,\mathrm{K}) = 1{,}551\,\mathrm{mN\cdot m^{-1}}$, with a temperature coefficient

$d\gamma/dT = -0.38\,\text{mN}\cdot\text{m}^{-1}\,\text{K}^{-1}$. The value of the CMSX-4® alloy calculated by Eq. 1 at the same temperature is $\gamma(1{,}913\,\text{K}) = 1{,}628\,\text{mN}\cdot\text{m}^{-1}$. As the CMSX-4® alloy is a Ni-based multicomponent alloy, its surface tension should be close to that of Ni, which is $\gamma_{\text{Ni}} = 1{,}760\,\text{mN}\cdot\text{m}^{-1}$[23] at $T = 1{,}913\,\text{K}$. On the other hand, the CMSX-4® alloy contains ≈12 at% Al having a surface tension close to $\gamma_{\text{Al}} = 720\,\text{mN}\cdot\text{m}^{-1}$ [21, 24] at the relevant temperature. Accordingly, the surface tension of the CMSX-4® alloy should therefore be lower than that of Ni. Moreover, the presence of metals having a surface tension higher than that of Ni together with several refractory metals (≈6 at%) in the CMSX-4® alloy as minor components, justifies the high surface tension obtained by the sessile-drop experiments. Furthermore, two other factors have to be taken into account: (a) a possible contribution of Al-vapor pressure ($P_{\text{Al}} = 36.9\,\text{Pa}$ at $T = 1{,}773\,\text{K}$) [25], although the observed mean mass loss of the samples during the sessile-drop experiments was not higher than 1%, which is also confirmed by the slight deviations of the density values and (b) the possible formation of different intermetallic compounds. In fact, all Al–X subsystems (X = Ni, Co, Cr, Ti, Mo, W, Re) [26] are compound forming alloys, and CMSX-4® as the combination of these systems (Table 1) is of the same type. So the presence of intermetallics in the solid state and of clusters with the same stoichiometry in the liquid phase has to be taken into account [27]. Accordingly, the theoretical evaluation of the surface tension of the CMSX-4® alloy has been done in Sect. 5.

3 Density

The density of the CMSX-4® liquid alloy was measured as a function of temperature by a levitation technique. Density measurements have been also performed by the sessile-drop method. The experimental values obtained by the two different techniques were compared with each other, and with the values calculated by different methods.

3.1 Measurement of Density

The density has been measured by a levitated-drop method, in which the volume of a droplet of known mass is determined from digital images obtained while it is suspended in an electromagnetic field. The apparatus (Fig. 4) consists of a turntable chamber at the bottom to hold a number of samples, a sealed pushrod which raises a sample into a square, and an optically flat sided tube which acts as an environmental chamber. An opposing turn levitation coil surrounds the tube. When an rf current (220 kHz) is applied to the coil, the sample levitates and is heated. The temperature is monitored by a two-color (0.9 and 1.1 μm) pyrometer, and controlled by varying the mixture of two gases of differing thermal conductivity (usually Ar and He or H_2) flowing through the apparatus. Digital cameras are placed in three planes around the sample to record images of the droplet simultaneously, so as to freeze any motion of the drop. Initially, a ball bearing of known diameter is placed in the tube and photographed in order to scale the subsequent images. Samples are weighed and placed on the turntable. After purging with gas, each sample is levitated and heated to a stable temperature, then a series of images are recorded. The samples are then cooled and reweighed. Images

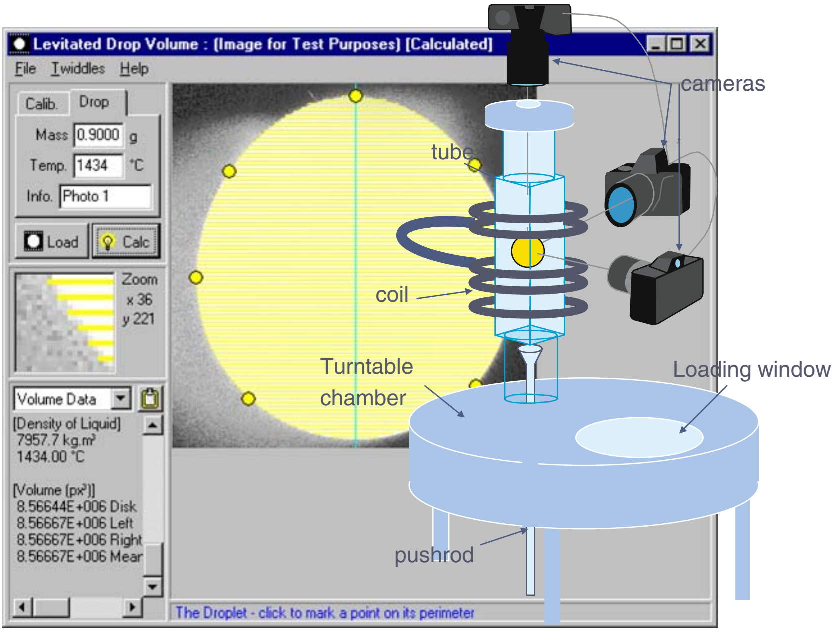

Mass 0.9000 g
Temp. 1434 °C
Info. Photo 1
Zoom x 36 y 221

[Density of Liquid]
7957.7 kg.m³
1434.00 °C

[Volume (px³)]
8.56644E+006 Disk
8.56667E+006 Left
8.56667E+006 Right
8.56667E+006 Mear

The Droplet - click to mark a point on its perimeter

Fig. 4 Apparatus for density measurements (NPL)

from the top camera are reviewed, and all images with a circular cross section are selected. The corresponding side views are scaled from the image of the ball bearing, and analyzed to determine the edge of the drop, the axis of symmetry, and, from radii taken along the axis, volumes of revolution. These are summed to give the total volume of the drop, and from the mean mass of the sample, the density is derived.

The density has been also measured by the sessile-drop technique applying the same methodology used for the determination of the surface tension described in Sects. 2.1 and 2.2. The density of the CMSX-4® alloy was calculated from the drop mass and volume measured at each temperature obtained during the automatic acquisition procedure. In this case, the uncertainty in the density values is estimated to be ±0.1%.

3.2 Density Measurement Results

The results of density measurements of the CMSX-4® in the temperature range between 1,654 and 1,843 K are shown in Fig. 5, together with the calculated values as described in Ref. 18. Applying the linear regression law to the experimental density data, the relationships between density and temperature can be expressed as

$$\rho_{\mathrm{LD}}(T)[\mathrm{kg}\cdot\mathrm{m}^{-3}] = 7{,}781 - 0.41(T - 1{,}654\,\mathrm{K}) \tag{3}$$

$$\rho_{\mathrm{SD}}(T)[\mathrm{kg}\cdot\mathrm{m}^{-3}] = 7{,}880 - 1.32(T - 1{,}654\,\mathrm{K}) \tag{4}$$

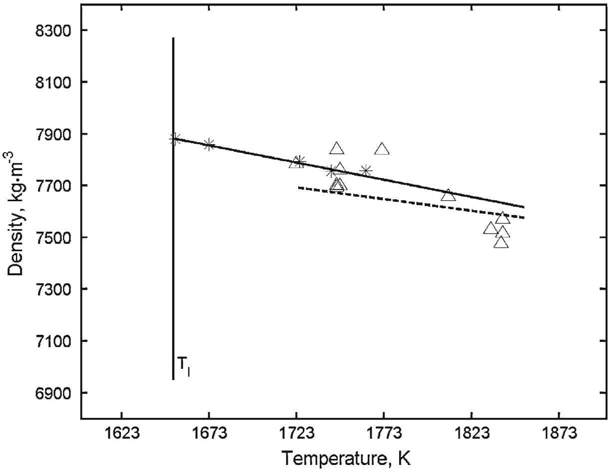

Fig. 5 Density of the CMSX-4® alloy as a function of temperature: (△) levitated drop; (∗) sessile drop; solid line: fit of experimental data; broken line: calculated values [18]. T_l is referred to as the melting temperature

The results obtained by the sessile-drop ($_{\text{SD}}$) experiments are in agreement with those obtained by the levitated-drop ($_{\text{LD}}$) experiments. In fact, where the temperature ranges overlap, the results obtained from both experiments agree to better than 1.5%. When the two sets of experimental data are combined, a recommended relationship of the density of the liquid CMSX-4® alloy, over the temperature range 1,654–1,843 K is obtained:

$$\rho(T)[\text{kg} \cdot \text{m}^{-3}] = 7{,}876 - 1.23(T - 1{,}654\,\text{K}) \tag{5}$$

Recently [10], a relationship between density and temperature for the CMSX-4® liquid alloy has been recommended, on the basis of density measurements performed by a modified pycnometric method:

$$\rho_{\text{py}}(T)[\text{kg} \cdot \text{m}^{-3}] = 7{,}740 - 0.87(T - 1{,}660\,\text{K}) \tag{6}$$

The results obtained by this method yield density values lower by 2% with respect to those obtained by the sessile-drop method, which is a comparable method. An explanation of this discrepancy is probably two-fold, i.e., the accuracy of the measurements and the differences in the alloy composition.

A theoretical estimation of the CMSX-4® density as a function of temperature can be done following the calculation described in Ref. 18 on the basis of Vegard's rule:

$$\rho_{\text{CALC}}(T)[\text{kg} \cdot \text{m}^{-3}] = 7{,}576 - 0.99(T - 1{,}654\,\text{K}) \tag{7}$$

Keeping in mind that the approach [18] is recommended for regular alloys [28], when applied to compound-forming alloys, such as CMSX-4®, the proposed density–temperature relationship can be only taken as the first approximation. Another model was suggested by Mills [29] giving the theoretical relationship between density and temperature, as follows:

$$\rho_{\mathrm{M}}(T)[\mathrm{kg}\cdot\mathrm{m}^{-3}] = 7{,}754 - 0.9(T - 1{,}654\,\mathrm{K}) \tag{8}$$

In this case, the deviation between the measured data and the calculated values was less than 1.5%.

4 Viscosity

Measurements of the viscosity of CMSX-4® were performed at the National Physical Laboratory using an oscillating-cup viscometer [30]. A cylinder of liquid, contained in a crucible suspended on a wire, is oscillated axi-symmetrically. After initiation of the oscillations, the rate of decay is measured. The main advantages of the method are that the time period and decrement are easily measured and the amount of liquid is relatively small which allows stable temperature profiles to be attained. One of the major difficulties is relating the measured parameters to the viscosity through the Roscoe equation [31].

Figure 6 shows the overall design of the oscillating viscometer. The sample is contained within an alumina crucible with an alumina lid, screwed to the end of a molybdenum suspension rod and Pt-8%W torsion wire. A rotary solenoid is connected to the wire to set the system oscillating. The suspension wire is contained within a water jacket maintained at 303 K. Above the suspension rod and below the wire is mounted a flat mirror, and a window within the jacket wall allows a 1 mW laser to shine directly at the mirror. The reflected light from the mirror is detected by an array of 40 light-sensitive diodes arranged in an arc ($\sim 60^\circ$) of a circle. The output voltages from the diode array are recorded by a computer, which can then reconstruct the oscillations as a sine wave, and by use of a downhill simplex algorithm, the logarithmic decrement of the oscillation can be derived. A two-zone furnace with an extensive uniform hot zone for temperatures up to 1,650 K is used to heat the specimen. A close-ended alumina work tube is used to enclose the crucible, and a graphite radiation/heat sink is situated above the crucible. The presence of the graphite helps to reduce the oxygen potential in the flowing Ar-atmosphere. The measurements were carried out in a series of steps in which the temperature was allowed to equilibrate. A measurement uncertainty of ±9% within a 95% confidence limit is claimed, which is principally contributed to the extrapolation of the dimensions of the crucible and the height of the liquid at high temperatures [32].

4.1 Viscosity Results

The results of the measurements performed are shown in Fig. 7, and are compared to measurements also made at NPL on pure nickel and IN718, another commonly used nickel superalloy. Individual measured points are shown, five of which were taken at each temperature. At higher temperatures, above 1,760 K, the data show more scatter than at lower temperatures. This is likely to be due to instabilities of the suspension

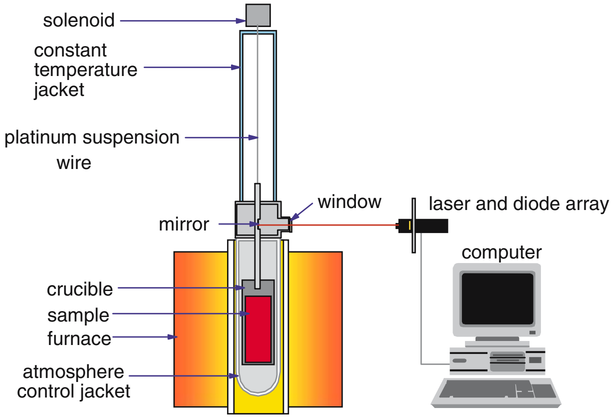

Fig. 6 Oscillating viscometer (NPL)

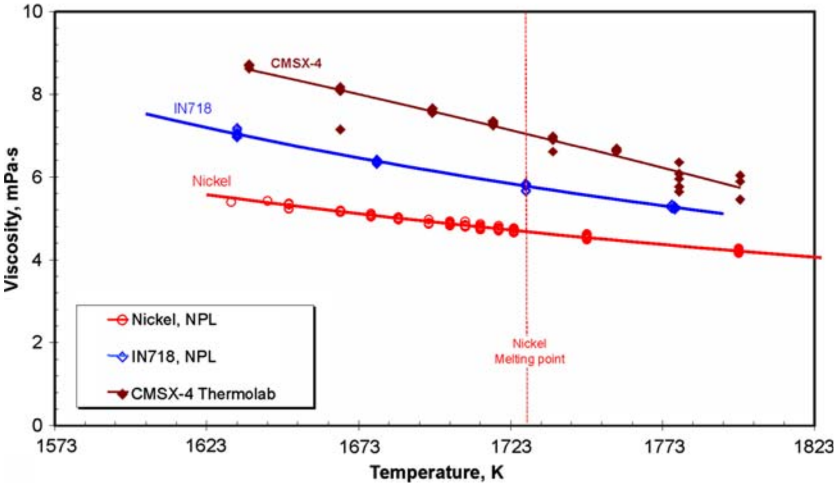

Fig. 7 Viscosity of the CMSX-4® alloy (♦) as a function of temperature compared with viscosity data of IN718 (◊) and Ni (○)

system during the initial measurements rather than a thermochemical effect, as these were made prior to the measurements below 1,760 K. The sample exhibited undercooling of 15 K, allowing a measurement to be made at 1,640 K, where the sample was fully liquid. However, the sample was predominantly solid by 1,620 K when a further measurement was attempted. Although the viscous behavior of metals is a thermally activated process, and usually an Arrhenius behavior is observed, the experimental data obtained in this study, over the temperature range measured, can be adequately described by a linear regression of the following form:

$$\eta(T)[\text{mPa} \cdot \text{s}] = 8.36 - 1.82 \times 10^{-2}(T - 1{,}654\,\text{K}) \tag{9}$$

It was not possible, with the amount of material available in this study, to make further measurements at higher temperatures, and thus discover where a nonlinear relation could be observed. However, the results are consistent with the trends shown in other measurements on nickel at NPL, as Fig. 7 shows how increasing the complexity of the composition in the alloy increases the viscosity.

5 Modeling of the Surface Tension

Due to difficulties to obtain reliable experimental data on thermophysical properties of liquid alloys at high temperatures, the prediction of these data is often necessary. In such case, it is possible to predict property values analyzing the dominant ternary system and/or its binary subsystems formed by the main components of a multicomponent system and taking into account the influence of minority components on that property. Accordingly, to address correctly the definition of thermophysical properties of the CMSX-4® alloy the Al–Ni system was taken as a model system for the industrial alloy [16].

Many alloys characterized by the formation of intermetallic phases in the solid state with different solubility limits, exhibit in the liquid phase an associative tendency among the unlike constituent elements. The compound formation model (CFM) [33] for binary systems takes into account the effects of short-range-order phenomena on the surface (surface tension and surface segregation) and the transport properties (diffusivity, viscosity) as well as on the microscopic functions (concentration fluctuations in the long wavelength limit and Warren–Cowley short-range-order parameter) [27]. The mixing properties of such molten alloys deviate from the regular solution behavior and show a well-defined peak at one or more concentrations, which lie in the vicinity of the stoichiometric compositions of energetically favoured intermetallic compounds. However, the predictive power of this model, and of nearly all thermodynamic models for the description of macroscopic thermophysical properties depend on a knowledge of the interaction energy parameters which are rarely known and have to be adjusted using thermodynamic data.

5.1 Surface Properties of Binary Liquid Alloys: CFM and Regular Solution Model

The generalized CFM formalism treats an alloy as a pseudo-ternary mixture of A atoms, B atoms, and $A_\mu B_\nu$ (μ and ν are small integers) groups of atoms or clusters with the stoichiometry of the intermetallics present in the solid state, all in chemical equilibrium with one another [27,34]. The absence of clusters in the melt reduces the model to the quasi-chemical approximation (QCA) for a regular solution. Butler's concept of a layered interface structure and the relationship between the component's activity in the bulk and the surface phase are basic hypotheses of both models [35]. The CFM formalism in the strong interaction approximation has been successfully applied to the Al–Ni system to describe the surface properties in the liquid state with respect to the AlNi, taken as an energetically favoured intermetallic compound. Many details on the calculations of thermodynamic and thermophysical properties of liquid binary alloys based on AB-stoichiometry ($\mu = 1$, $\nu = 1$) in the framework of the CFM have been previously reported [33,36]. In the present work only two basic equations used for the calculation of the surface-tension isotherms are given. The surface tension for compound forming alloys can be expressed as:

$$\begin{aligned}\gamma = \gamma_{\mathrm{A}} + \frac{k_{\mathrm{B}}T}{\alpha}\ln\frac{C^{\mathrm{s}}}{C} + \frac{W}{\alpha}\left[p\left(f^{\mathrm{s}} - f\right) - qf\right]\\ + \sum_{i,j=\mathrm{A,B}}\frac{\Delta W_{ij}}{\alpha}\left[p\left(f_{ij}^{\mathrm{s}} - f_{ij}\right) - qf_{ij}\right]\end{aligned} \tag{10a}$$

$$\begin{aligned}\gamma = \gamma_{\mathrm{B}} + \frac{k_{\mathrm{B}}T}{\alpha}\ln\frac{(1-C^{\mathrm{s}})}{(1-C)} + \frac{W}{\alpha}\left[p\left(\phi^{\mathrm{s}} - \phi\right) - q\phi\right]\\ + \sum_{i,j=\mathrm{A,B}}\frac{\Delta W_{ij}}{\alpha}\left[p\left(\phi_{ij}^{\mathrm{s}} - \phi_{ij}\right) - q\phi_{ij}\right]\end{aligned} \tag{10b}$$

where γ_{A} and γ_{B} are surface tensions of components A and B, respectively. C and C^{s} are bulk and surface concentrations of A, while W and ΔW_{ij} are interaction energy parameters. k_{B}, T, p, and q are Boltzman's constant, absolute temperature, and surface coordination fractions, respectively. α is the mean surface area of the alloy. The equations for surface tension derived by the CFM (Eqs. 10a and 10b) include the concentration functions ϕ, ϕ_{ij}, f_{ij}, ϕ^{s}, ϕ_{ij}^{s}, and f_{ij}^{s}.

The surface tension described by the QCA for regular solution, is given by

$$\begin{aligned}\gamma = \gamma_{\mathrm{A}} + \frac{k_{\mathrm{B}}T(2-pZ)}{2\alpha}\ln\frac{C^{\mathrm{s}}}{C}\\ + \frac{Zk_{\mathrm{B}}T}{2\alpha}\left[p\ln\frac{(\beta^{\mathrm{s}}-1+2C^{\mathrm{s}})(1+\beta)}{(\beta-1+2C)(1+\beta^{\mathrm{s}})} - q\ln\frac{(\beta-1+2C)}{(1+\beta)C}\right]\end{aligned} \tag{11a}$$

$$\begin{aligned}\gamma = \gamma_{\mathrm{B}} + \frac{k_{\mathrm{B}}T(2-pZ)}{2\alpha}\ln\frac{(1-C^{\mathrm{s}})}{(1-C)}\\ + \frac{Zk_{\mathrm{B}}T}{2\alpha}\left[p\ln\frac{(\beta^{\mathrm{s}}+1-2C^{\mathrm{s}})(1+\beta)}{(\beta+1-2C)(1+\beta^{\mathrm{s}})} - q\ln\frac{(\beta+1-2C)}{(1+\beta)(1-C)}\right]\end{aligned} \tag{11b}$$

where β and Z are an auxiliary variable and the coordination number, respectively [27]. In all equations the superscript s indicates the surface phase. The application of both models, the CFM and the QCA for regular solutions, makes it possible to estimate the effect of short-range-order phenomena on the surface tension, expressed by the difference between the property values calculated by the two models.

5.2 Theoretical Evaluation of the Surface Tension

The study of the surface properties of multicomponent alloys, such as CMSX-4®, should take into consideration the corresponding properties of its subsystems

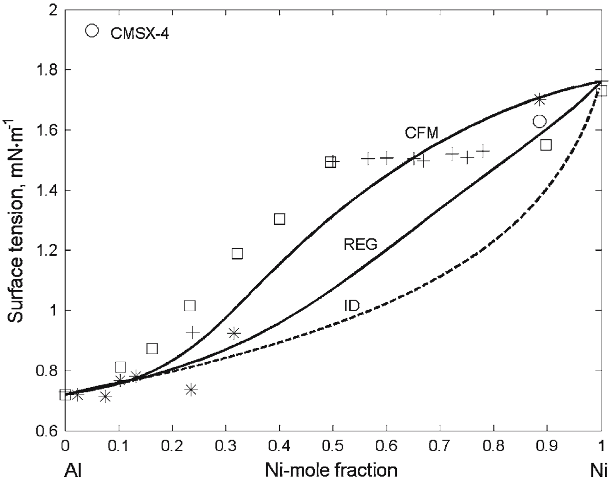

Fig. 8 Experimental values of the surface tension of CMSX-4 alloy (○) together with calculated surface-tension isotherms of Ni–Al alloys (CFM = compound formation model; REG = regular solution model; ID = ideal solution) and experimental data: (+) [14]; (□) [15]; (∗) sessile drop [16], at $T = 1{,}913\,\mathrm{K}$

(binaries and ternaries) formed by the principal alloy components. Accordingly, Al–Ni [16], Al–Co, Co–Ni [36] and Al–Co–Ni [37] have been analyzed in detail. Once these systems were elaborated, the influence of the other alloy components (Table 1) has been considered with respect to the dominant subsystem, Al–Ni.

In order to compare the experimental results of CMSX-4®, the surface-tension measurements of the Al-88.6 at% Ni liquid alloy were also performed. Both alloys have the same Al-content, and the last one yields an estimate of the CMSX-4® surface tension in terms of a lower limit, approximating an overall contribution of refractory metals from that of nickel.

Taking into account that the Al–Ni system belongs to compound forming alloys, the mixing behavior of these alloys is certainly better described by the CFM as compared to the REG. The AlNi intermetallic phase exists up to 1,911 K, its composition, C_{Ni}, varies between 0.42 and 0.68 [26,38], and it was taken as energetically favoured in our calculations. The input data were the thermodynamic data of the Al–Ni liquid phase [38] together with the surface tension reference data of pure Al [21,24] and pure Ni [23].

All experimental data on the surface tension of liquid Al–Ni alloys together with the CMSX-4® value measured at 1,913 K as well as the surface-tension isotherms calculated by the CFM (Eqs. 10a and 10b) and QCA for regular solutions (REG) (Eqs. 11a and 11b) are shown in Fig. 8. The contribution of the short-range-order to the surface tension of liquid Al–Ni alloys has been estimated by the difference in the surface tension calculated by the two models. As shown in Fig. 8, for the alloys with compositions close to those of energetically favoured intermetallic compounds, the presence of associates or clusters in the liquid phase increases the surface tension up to 10%.

The surface-tension isotherm calculated by the CFM exhibits a strong irregularity near the compositions that correspond to intermetallic compound concentrations, and agrees fairly well with the experimental data reported in the literature [15,16]. On the contrary, the data reported by Eremenko et al. [14] exhibit an anomalous trend. The experimental surface-tension data of the Al-88.6 at% Ni and the CMSX-4® determined in this work exhibit good agreement with the theoretical values obtained by the CFM.

6 Conclusions

The surface tension, density, and viscosity of the CMSX-4® superalloy have been determined in the temperature ranges of 1,650–1,950 K, 1,650–1,850 K, and 1,623–1,800 K, respectively.

The viscosity values are of comparable order to those of similar Ni-based alloys, but higher than data reported in the literature. The experimental data as a function of temperature can be adequately described using a linear regression law. The low scatter in the data at the lower temperatures demonstrates the repeatability of the measurements. The lack of viscosity data on CMSX-4® as well as the lack of a second reliable method, which may be used to validate the oscillating cylinder method, means that the data stand on their own merit.

Similar conclusions can be made for the density data. The experimental results obtained from different methods are in good agreement with each other and agree fairly well with the calculated values, so that the density of liquid CMSX-4® alloy can be reliably described by the proposed relationship.

Good agreement was also found between the surface-tension experimental data obtained by the sessile-drop method with different techniques. The surface-tension experimental data of liquid CMSX-4® alloy can be reliably described by the proposed relationship, and they were found to be in good agreement with those of the Al-88.57 at% Ni alloy having the same Al-content.

The presence of high melting metals, such as Co, Mo, Ta, Re, and W with surface-tension values significantly higher than that of Ni, justifies the high surface-tension values observed for this multicomponent alloy as well as the contradictory results obtained by other methods. A further confirmation of this achievement represents very good agreement between the surface-tension values obtained in this work and those predicted by thermodynamic model calculations.

Acknowledgments The contributions of CNR-IENI, KTH, and NPL have been realized in the framework of the MAP "ThermoLab-Project": ESA financial support is gratefully acknowledged. Authors wish to thank the entire ThermoLab team for fruitful discussions.

References

1. V. Naidich, *Progress in Surface and Membrane Science,* vol. 14 (Academic Press, New York, 1981), p. 353
2. N. Eustathopoulos, M. Nicholas, B. Drevet, *Wettability at High Temperatures* (Pergamon Materials Series, Oxford, UK, 1999)
3. B.J. Keene, Int. Mater. Rev. **38**, 157 (1997)
4. B.J. Keene, DMM(A) **113**, (1993)
5. A. Jakobsson, M. Nasu, J. Mangwiru, K.C. Mills, S. Seetharaman, Phil. Trans. R. Soc. Lond. A **356**, 995 (1998)
6. R.F. Brooks, B.J. Monaghan, A.J. Barnicoat, A. McCabe, K.C. Mills, P.N. Quested, Int. J. Thermophys. **17**, 1151 (1996)

7. E. Ricci, E. Arato, A. Passerone, P. Costa, Adv. Colloid Interface Sci. **117**, 15 (2005)
8. B. Vinet, S. Schneider, J.P. Garandet, B. Marie, B. Drevet, I. Egry, Int. J. Thermophys. **25**, 1889 (2004)
9. M. Hayashi, A. Jakobsson, T. Tanaka, S. Seetharaman, High Temp.-High Press. **35/36**, 441 (2003)
10. Z. Li, K.C. Mills, M. McLean, K. Mukai, Metall. Mater. Trans. B **36B**, 247 (2005)
11. R. Wunderlich, H. Fecht, Meas. Sci. Technol. **16**, 402 (2005)
12. C. Maze, G. Burnet, Surf. Sci. **13**, 451 (1969); Surf. Sci. **24**, 335 (1971)
13. L. Liggieri, A. Passerone, High Temp. Technol. **7**, 80 (1989)
14. V.N. Eremenko, V.I. Nizhenko, Yu.V. Naidich, Izv. Akad. Nauk SSSR, Metallurgiya i Topivo **3**, 150 (1961)
15. J.G.D. Ayushina, E.S. Levin, P.V. Gel'dovich, Russ. J. Phys. Chem. **43**, 1548 (1969)
16. R. Aune, L. Battezzati, I. Egry, J. Etay, H.J. Fecht, D. Giuranno, R. Novakovic, A. Passerone, E. Ricci, F. Schmidt-Hohagen, S. Seetharaman, R. Wunderlich, Microgravity Sci. Technol. **XVIII-3/4**, 5 (2006)
17. K.F. Lin, C.C. Lin, Scripta Mater. **39**(10), 1333 (1998)
18. T. Iida, R.I.L. Guthrie, *The Physical Properties of Liquid Metals* (Clarendon Press, Oxford, 1993)
19. E. Ricci, A. Passerone, J.C. Joud, Surf. Sci. **206**, 533 (1988)
20. E. Ricci, D. Giuranno, E. Arato, P. Costa, in *5th Int. Conf. on High Temp. Capillarity*, HTC 2007, March 21–24, Alicante, Spain (2007)
21. J.M. Molina, R. Voytovvch, E. Louis, N. Eustathopoulos, Int. J. Adhes. Adhes. **27**, 394 (2007)
22. K.C. Mills, *Recommended Values of Thermophysical Properties for Commercial Alloys* (Woodhead Pub., Cambridge, United Kingdom, 2002)
23. J.V. Naidich, V.M. Perevertailo, G.M. Nevodnik, Russ. Metall. **2**, 66 (1972)
24. G. Lang, P. Laty, J.C. Joud , P. Desré, Z. Metallkd. **68**, 113 (1977)
25. O. Knacke, O. Kubashewski, K. Hesselmann, *Thermochemical Properties of Inorganic Substances* (Springer Verlag, Duesseldorf, 1991)
26. T.B. Massalski, *Binary Alloy Phase Diagrams* (Am. Soc. for Metals, Materials Park, Ohio, 1986)
27. R.N. Singh, N.H. March, in *Intermetallic Compounds, Principles and Practice*, ed. by J.H. Westbrook, R.L. Fleischer (John Wiley & Sons, Chichester, UK, 1995)
28. W. Hume-Rothery, P.W. Reynolds, J.V. Raynor, *J. Inst. Metals* **66**, 191 (1940)
29. K.C. Mills, Y.M. Youssef, Z.S. Li, ISIJ Int. **46**, 623 (2006)
30. R. Brooks, A.P. Day, R.J.L. Andon, L.A. Chapman, K.C. Mills, P.N. Quested, High Temp.-High Press. **33**, 73 (2001)
31. R. Roscoe, Proc. Phys. Soc. **72**, 576 (1958)
32. R. Brooks, I. Egry, E. Ricci, S. Seetharaman, R. Wunderlich, High Temp. Mater. Proc. **25**, 303 (2006)
33. R. Novakovic, E. Ricci, F. Gnecco, D. Giuranno, G. Borzone, Surf. Sci. **599**, 230 (2005)
34. A.B. Bhatia, W.H. Hargrowe, D.E. Thornton, Phys. Rev. B **9**, 435 (1974)
35. J.A.V. Butler, Proc. R. Soc. A **135**, 348 (1932)
36. R. Novakovic, T. Tanaka, Physica B **371**, 223 (2006)
37. R. Novakovic, E. Ricci, *Surface Properties of the Al–Co–Ni System* (Calphad XXXI, Stockholm, Sweden, 2002)
38. N. Dupin, *Contribution à l'évaluation thermodynamique des alliages polyconstitués à base de nickel* (Ph.D. thesis, Institut National Polytechnique de Grenoble, 1995)